



## Short communication

# Polymer electrolyte membrane fuel cell performance degradation by coolant leakage and recovery

Ju Hae Jung <sup>a</sup>, Se Hoon Kim <sup>a</sup>, Seung Hyun Hur <sup>a</sup>, Sang Hoon Joo <sup>b</sup>, Won Mook Choi <sup>a</sup>, Junbom Kim <sup>a,\*</sup>

<sup>a</sup> School of Chemical Engineering & Bioengineering, University of Ulsan, Ulsan, 680-749, Republic of Korea

<sup>b</sup> School of Nano-Bioscience and Chemical Engineering, Ulsan National Institute of Science and Technology (UNIST), UNIST-gil 50, Ulsan 689-798, Republic of Korea

## HIGHLIGHTS

- Performance behavior by coolant leakage was studied in the PEMFC.
- Performance degradation showed only at anode of 3-cell stack after coolant injection.
- The performance of unit cell was easily reduced in short intervals and large dose of coolant injection.
- The reduced performance was recovered over 90% by water injection.
- The performance of exposed GDL was recovered by water cleaning, but the performance of exposed MEA was not.

## ARTICLE INFO

### Article history:

Received 22 June 2012

Received in revised form

22 September 2012

Accepted 12 October 2012

Available online 7 November 2012

### Keywords:

Polymer electrolyte membrane fuel cell

Degradation

Coolant

Ethylene glycol

Carbon monoxide poisoning

## ABSTRACT

Coolant leakage leads to decrease in performance during the operation of electric vehicles which make use of polymer electrolyte membrane fuel cells (PEMFC). This study examines the effects of various coolant leak conditions in 3-cell stack and single cell. The experimental results show that an irreversible reduction in performance occurs after coolant injection into the anode side of the stack. Poisoning of carbon monoxide (CO) on the platinum (Pt) catalyst is caused by electro-oxidation reaction of EG. Water cleaning is selected because CO poisoning is desorbed to reaction with water molecules. Performance is quickly reduced when the interval between coolant injections is short. Performance reduction is indicated by the experimental results for the gas diffusion layer (GDL) and the membrane electrode assembly (MEA). It shows that performance of the MEA with the GDL exposed to coolant decreased, but it is recovered after water cleaning. In contrast, results for performance of the MEA exposed to coolant for long time could not be reversed after water cleaning. Therefore, we propose that performance degradation of coolant leak on the Pt catalyst surface and GDL can be recovered by the water cleaning simply without disassembly of stack.

© 2012 Elsevier B.V. All rights reserved.

## 1. Introduction

Energy dependence on fossil fuels is increasing rapidly, and research related to the environmental impact of conventional energy production from fossil fuels has greatly expanded. Efficient methods to produce energy are currently being developed, such as polymer electrolyte membrane fuel cell (PEMFC), which holds a great deal of promise as an energy source for producing clean energy from renewable resources. PEMFCs are also an attractive alternative for use in electrically powered automobiles, homes, and portable devices. The development of a fuel cell vehicle has been

accelerated due to increased concerns about environmental problems, including global warming caused by carbon dioxide emissions and air pollutants from excessive consumption of fossil fuels [1–7].

PEMFCs have many advantages, such as high efficiency, high power density, low-temperature operation, fast start-up, good system reliability, transient responsiveness, and zero emissions [8–10]. Additional benefits include low volume, easy scalability, and mobility. PEMFCs have no friction-induced energy loss because they have no mechanical moving parts like those of the internal combustion engine, thus its power generation efficiency is high, at 80% [11–13].

Electricity and water are produced by an electrochemical reaction between hydrogen and oxygen in the PEMFC. This reaction also generates heat. If the temperature of the PEMFC stack is increased to 100 °C, the PEMFC performance is decreased due to

\* Corresponding author. Tel.: +82 522592833; fax: +82 522591689.

E-mail address: [jbkим@ulsan.ac.kr](mailto:jbkим@ulsan.ac.kr) (J. Kim).

reduced ionic conductivity caused by drying of the polymer electrolyte membrane. Currently, PEMFC stacks of tens or hundreds of cells in the kW-class are used as power sources in electric vehicles. To maintain a set temperature, the extra heat generated by the electrochemical reaction has to be removed from the fuel cell stack. Therefore, improving the cooling systems of PEMFCs is critical to increase the electric power generation of these cells [11,14,15].

Generally, ethylene glycol (EG) is used as a coolant in traditional engines. EG (bp 198 °C) can also be used to cool a fuel cell. The intermediates (glycolaldehyde, glyoxal, glycolic acid, glyoxylic acid, and oxalic acid) of EG oxidation on Pt catalysts were investigated by reflection infrared spectroscopy, coulometric and voltammetric measurements. Wieland et al. suggested that CO<sub>2</sub> and CO are generated when the C–C bond is broken by the oxidation of EG with Pt electrodes in an acidic environment [16]. The–CO molecule is formed from formaldehyde (methylene glycol) by methanol oxidation and leads to poisoning of the surface of the Pt catalyst. However, formaldehyde-generated CO poisoning was seen to occur on Pt–Sn catalysts in an oxygen-poor environment, while CO<sub>2</sub> was generated in an oxygen-rich environment [17]. By using a Pt–Ru alloy catalyst, the current of EG oxidation was increased and the generated CO<sub>2</sub> was decreased with increasing Ru concentration under acidic conditions [18].

K. Matsuoka et al. studied the electro-oxidation of polyhydric alcohol in alkaline solutions using a platinum electrode with an alkaline direct alcohol fuel cell. They showed that using EG as fuel provided the maximum power density. In addition, they found poisoning and non-poisoning paths of EG oxidation. The non-poisoning path of EG oxidation produced oxalate in an alkaline solution. Thus, the EG created much less poisoning than methanol on the Pt catalyst at 0.4 V [19,20]. J. D. Kim et al. investigated the effect of CO concentration and tolerance as a function of the cell temperature of PEMFCs. They found that cell impedance at low temperature and high CO concentration depended on anode impedance and that the cathode impedance was less affected by CO gas [21].

EG has the unfortunate property that it decomposes into CO gas, which results in poisoning of Pt catalysts and decreases the performance of PEMFCs and directs methanol fuel cells (DMFCs) [21–30]. When CO is injected in pulses with concentrations of more than 100 ppm, the cell voltage shows an oscillatory response, suggesting that cell performance can be recovered by cyclic injection of pure hydrogen [22]. B. Wu et al. explained that treating a surface with tetrahydrofuran and acetone increases the activity of Pt catalysts due to removal of the CO adsorbed on the Pt catalyst [23]. Furthermore, polyoxometalate-deposited Pt/C catalysts prevent CO poisoning [24]. The CO tolerance of the PEMFC can be increased by current pulsing, and the average cell potential and overall efficiency can be increased by periodic pulsed oxidation (CO removal) from the catalyst surface [25,26]. By using a reference cell, the effect of CO on performance could be controlled in terms of both anode and cathode voltages after CO gas was injected at the anode. The activation effect was improved by CO adsorption/CO<sub>2</sub> desorption cycles [27–29]. V. Livshits et al. studied the electro-oxidation of EG using direct ethylene glycol fuel cells (DEGFC). They discovered that EG was converted completely to CO<sub>2</sub> as measured using ion chromatography [30,31]. G. J. M. Janssen et al. studied the effects of CO<sub>2</sub> on PEMFCs by experiment and modeling. Formation of CO from the CO<sub>2</sub> created by the reverse water shift reaction caused performance to decrease [32,33]. In addition, electrical resistance can be increased by corrosion on the contact parts caused by EG infiltrating between the bipolar plate and the membrane electrode assembly (MEA). However, there have been few studies

to examine how the leak time and quantity of coolant (EG) affects the performance of the PEMFC, including the MEA. Therefore, the aim of this study was to investigate cell performance changes caused by various coolant leakage situations in stacks and single cells.

## 2. Experimental

### 2.1. Preparation of MEA and electrochemical evaluation

Commercial MEA, which has a platinum loading of 0.4 mg cm<sup>-2</sup> on both electrodes, was used. A felt-type gas diffusion layer (GDL, 10BB, SGL) was used. The stack had three single cells with an electrode area of 250 cm<sup>2</sup>. Ethylene glycol (EG) 99.5% was mixed at a 1:1 volume ratio with deionized water for use as a coolant.

Fig. 1 shows the experimental apparatus used in this study. For reactants, humidified hydrogen and air with 100% relative humidity were supplied to the anode and cathode at ambient pressure with stoichiometric ratios of 1.5 and 2.0, respectively. The temperature of the cell fixture and humidifier were maintained at 65 °C. Coolant was injected by micro syringe or micro pump. The micro pump had a flow rate of up to 1500 µl min<sup>-1</sup>. If a large decrease in performance under certain conditions was detected, deionized water was injected using a water-pump with N<sub>2</sub> gas at the same time. Water and nitrogen were injected into the single cell at 1.5 ml min<sup>-1</sup> and 0.1 L min<sup>-1</sup>, respectively.

### 2.2. Coolant leak test in stack and single cell

A three-cell stack was tested to determine changes in performance. If performance in any of the three cells was reduced to 0.4 V after injecting the coolant into the anode and cathode sides independently, coolant infusion was stopped. The experiment was performed in constant current mode at a 400 mA cm<sup>-2</sup> current density. If performance reduction was observed, recovery experiments were carried out at constant current. Experimental estimations of GDL and MEA, each exposed to coolant, were conducted independently. GDL experimental performance was evaluated by replacing the GDL exposed in coolant for 3 h with a fresh GDL at the activated anode side. MEA experimental performance was monitored by removing the anode GDL and exposing the anode electrode to coolant for 3 h. In order to confirm the results of this experiment, a reproducibility test was conducted for electrode loss when the GDL was replaced at the anode side. A constant current recovery test was conducted when performance decreased, and a distilled water cleaning process was conducted for the MEA when performance could not be recovered. The electrode area of the single cell used for this experiment was 25 cm<sup>2</sup>.

### 2.3. Physical and electrochemical analysis

The cell performance changes in the stack and single cell were measured using a polarization curve, electrochemical impedance spectroscopy (EIS, Gamry, PC14), and cyclic voltammetry (CV, WonAtech, GWPG100HP). The concentrations of EG were analyzed by a Hewlett Packard 5890 Series II gas chromatograph (GC) with a flame ion detector (FID). Contact angle, which is the vapor–liquid angle at the interface of the solid surface [34], was measured. Surface tension measurements were carried out from 20 °C to 80 °C by the Du Noüy ring method using a DST 60 tension meter (Surface Electro Optics Co. LTD) under atmospheric pressure. A DV-II Pro viscometer (Brookfield Engineering) was used to measure liquid viscosity between 20 °C and 80 °C using standard procedures. Each sample solution was stirred with a magnetic stirrer, and the

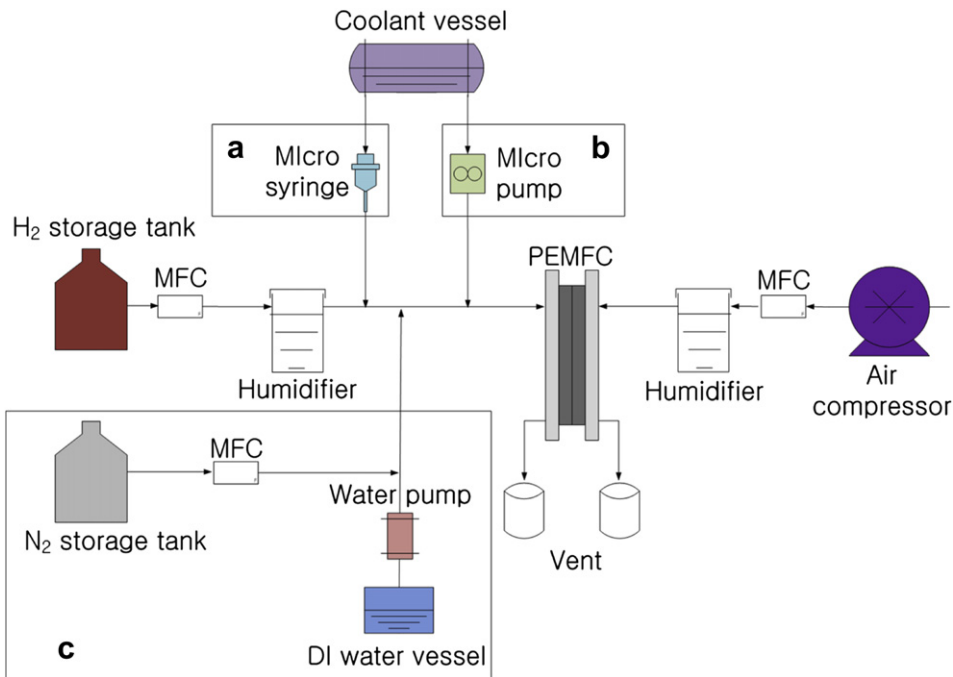


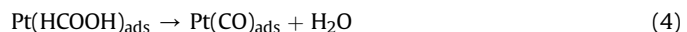
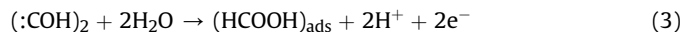
**Fig. 1.** Schematic diagram of experimental system (a) coolant injection using micro syringe (b) coolant injection using micro pump (c) recovery system using water.

surface tension was measured after the stirring had been discontinued for 3 min.

### 3. Results and discussion

#### 3.1. Stack evaluation during coolant leak

A 3-cell stack was tested for coolant leakage. The anode and cathode side behavior and performance were observed independently after injecting coolant. They were subsequently monitored in constant current (CC) mode for recovery. The results for injection of coolant at a rate of 0.5 ml min<sup>-1</sup> on the anode side under a constant current mode of 400 mA cm<sup>-2</sup> are shown in Fig. 2(a). The cell performance was reduced from 2.1 V to 1.2 V at 20 min after the injection of coolant. The results related to constant current recovery are shown in Fig. 2(b). The open circuit voltage (OCV) recovered somewhat in the stack, but the performance did not recover at a current density of 400-mA cm<sup>-2</sup>. The overpotential value was measured both anode and cathode by electro-oxidation reaction of EG [30]. Hence, the OCV and cell performance were reduced after coolant injection. As shown in Fig. 2(c), the cathode side was tested at the same coolant infusion rate and the same constant current mode. The performance repeatedly decreased and recovered, and was maintained at 1.9 V Fig. 2(d) shows the cell performance at a constant current mode at 400 mA cm<sup>-2</sup> after stopping the coolant injection. The cell performance recovered to its initial level in the cathode in constant current mode. The variations in the performance of the anode and cathode in the 3-cell stack are displayed in Fig. 3. In the anode (Fig. 3(a)), the initial performance was reduced by 43% after coolant injection, from 1050 mA cm<sup>-2</sup> to 600 mA cm<sup>-2</sup> at 1.8 V, and did not recover in CC mode. However, the cell performance in the cathode (Fig. 3(b)) decreased by 24% and recovered to 100% in CC mode. This is because water is generated by the reaction of protons, electrons, and oxygen in the cathode [11], which reduces the effect of the injection of coolant. A mechanism of EG oxidation is known as follows [37,38].



Adsorbed CO on Pt catalyst was oxidized to CO<sub>2</sub> by the dissociation of water molecules. Hence, water molecules are important for recovery of cell performance due to the electro-oxidation reaction of EG. The recovery at the anode was more difficult than at the cathode due to lack of water. Therefore, the experiments described in the following section were conducted to evaluate the effects of coolant injection on the anode. The water injection method was used to recover cell performance.

#### 3.2. Evaluation of single cells during coolant leakage

##### 3.2.1. Micro coolant injection experiments

Performance changes in the MEA at various leakage times and quantities of coolant were tested. In the first series, the amount of coolant in each injection was 0.5 µl min<sup>-1</sup> or 2.5 µl min<sup>-1</sup> (total quantity of coolant was 120 µl). The CV measurement results for 2.5 µl min<sup>-1</sup> injections are shown in Fig. 4. Compared with the initial measurement, the electrochemical catalyst surface area (ECSA) decreased by approximately 14.4%. This decrease in ECSA is likely caused by CO poisoning. In the oxidation of EG, CO is produced via several intermediate reactions, and this CO is adsorbed onto the Pt. It was confirmed by CV that the ECSA of the Pt electrode was decreased due to CO poisoning [23,26–28,32]. The resistance was measured using EIS to determine how resistance was affected by the injection of coolant at 400 mA cm<sup>-2</sup>, as shown

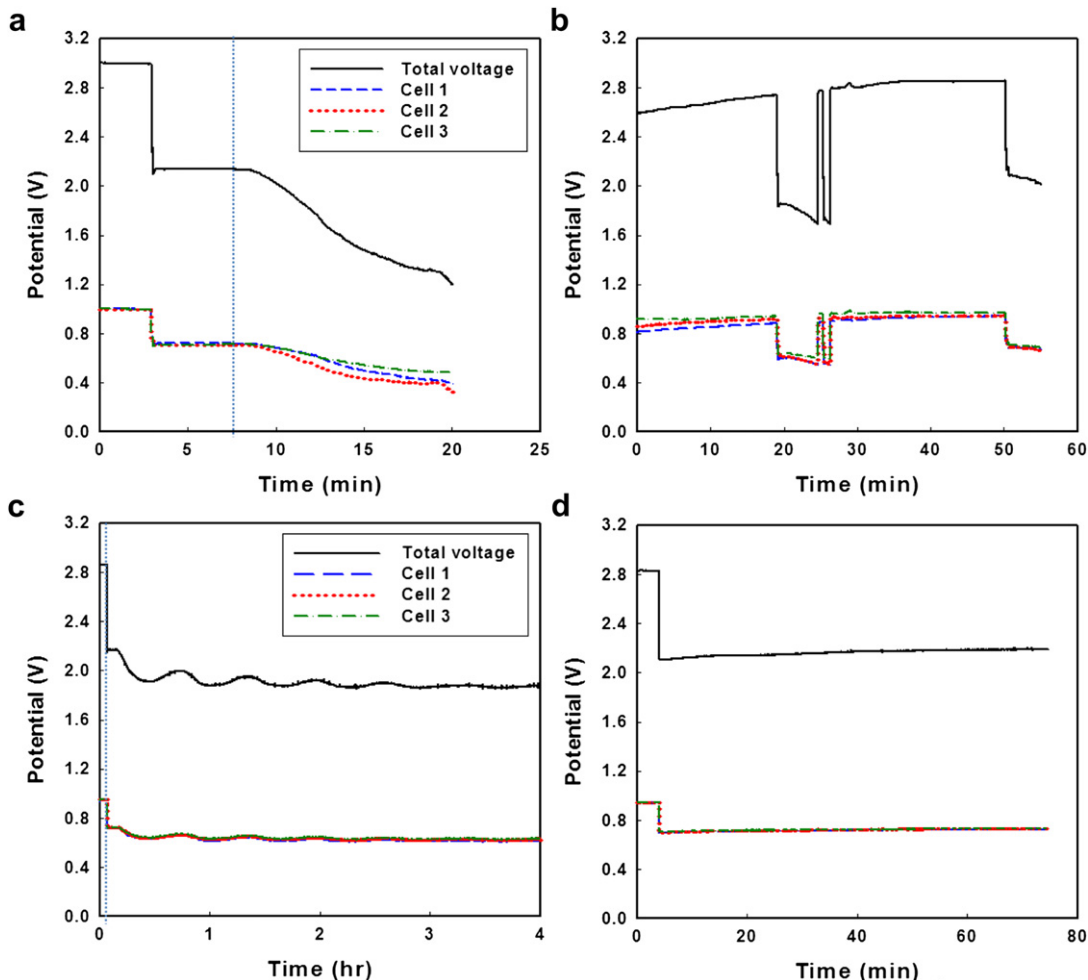


**Fig. 2.** Performance changes at constant current mode ( $400 \text{ mA cm}^{-2}$ ) by (a) coolant injection with  $0.5 \text{ ml min}^{-1}$  in anode, (b) CC mode recovery in anode, (c) coolant injection with  $0.5 \text{ ml min}^{-1}$  in cathode, and (d) CC mode recovery in cathode.

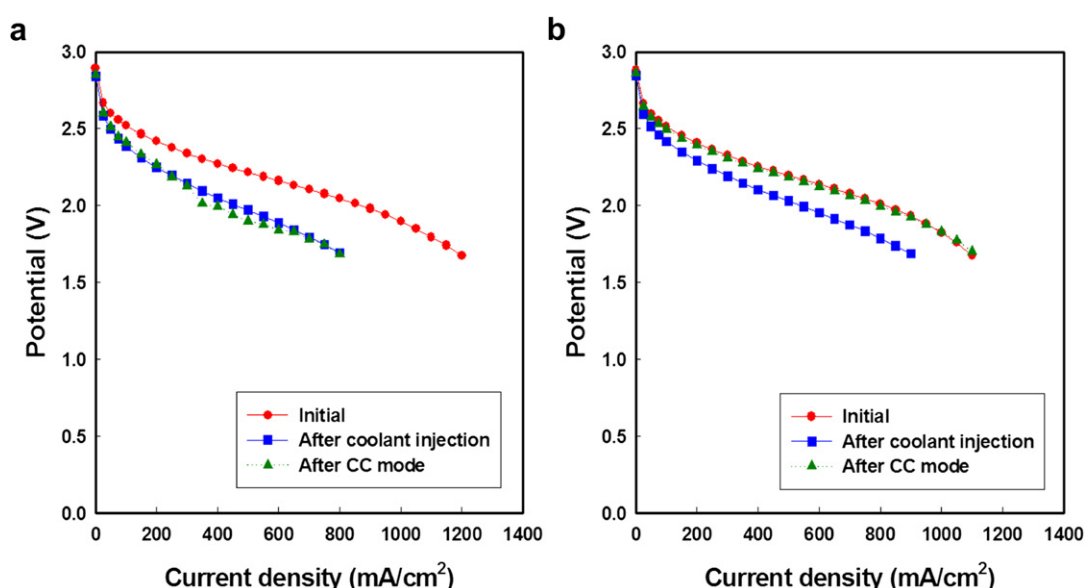


**Fig. 3.** Performance changes (a) at anode and (b) at cathode by coolant injection in the 3 cell stack.

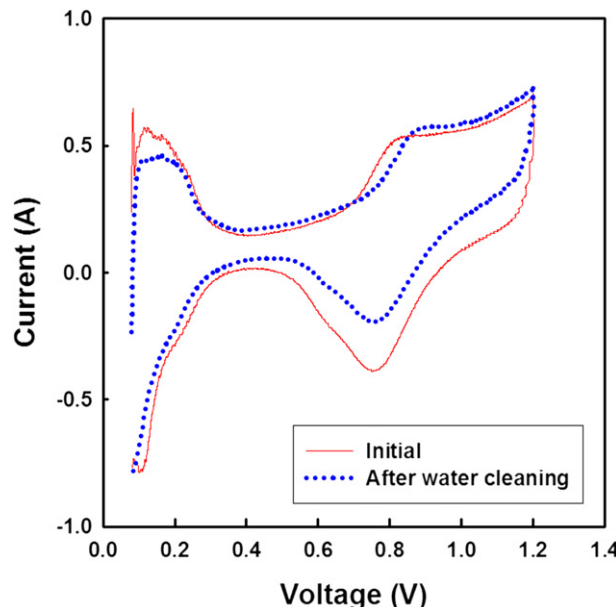


**Fig. 4.** Cyclic voltammogram changes of  $5 \mu\text{l}$  coolant injection at the anode in unit cell.

in Fig. 5. In the Nyquist plots, the diameter of the semicircle equals to the surface charge transfer resistance ( $R_{\text{ct}}$ ), which usually represents the resistance of electrochemical reactions on the electrode. This resistance is highly related to the active surface area of catalyst where the electrochemical reaction occurs. In addition, the polarization (overall) resistances are described as sum of the ohmic resistance, charge transfer resistance and mass transfer resistance. After coolant injection, the ohmic resistance ( $\Omega_{\text{ohm}}$ ) did not change, but polarization resistance ( $\Omega_{\text{pol}}$ ) increased to  $0.005 \Omega$ , and then decreased to  $0.02 \Omega$  after water cleaning. The polarization resistance difference was small between CC mode and water cleaning. It seems that cell performance was recovered after measurement of polarization curve and CV. J.D. Kim et al. similarly showed that polarization resistance ( $\Omega_{\text{pol}}$ ) is increased with increasing CO concentration, but ohmic resistance ( $\Omega_{\text{ohm}}$ ) was not

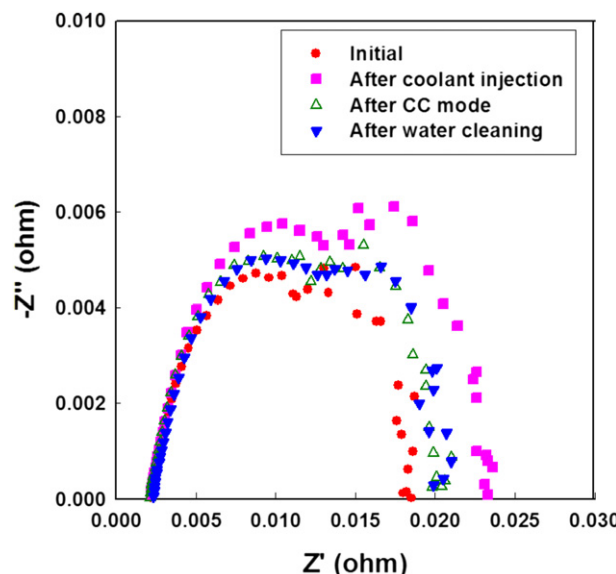


**Fig. 5.** Electrochemical impedance spectroscopy of  $2.5 \mu\text{l min}^{-1}$  coolant injection at current density of  $400 \text{ mA cm}^{-2}$  in unit cell.

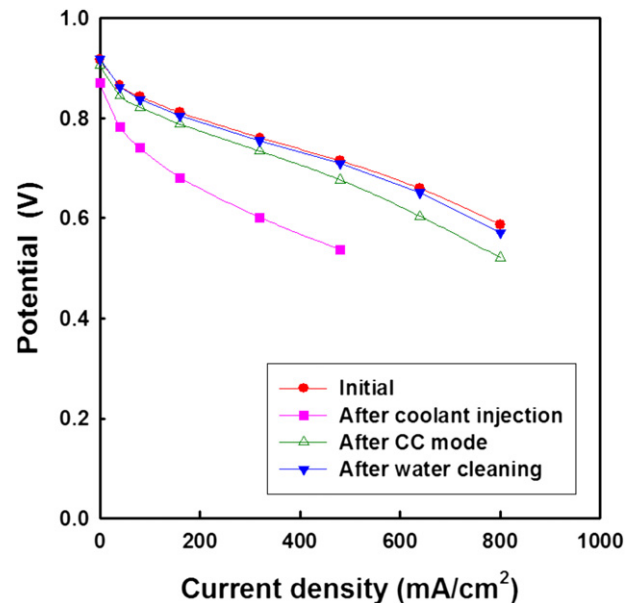


**Fig. 6.** Polarization curve changes of  $2.5 \mu\text{l min}^{-1}$  coolant injection in unit cell.

changed. Polarization resistance is directly related to cell performance [21]. The changes in the polarization curve are shown in Fig. 6. After the injection of the coolant, the OCV was decreased by 5.1%, and recovered completely in CC mode after water cleaning. The performance at  $0.6 \text{ V}$  was decreased by 58.2% from the initial performance after coolant injection, but recovered to 83.8% and 96.2% after recovery in CC mode and water cleaning, respectively. Table 1 represents the results after coolant injection of  $0.5 \mu\text{l min}^{-1}$ . The cell performance was recovered more than 95% by water cleaning. However, these results suggest that the reduction of ECSA cannot be avoided due to CO poisoning on the catalyst layer by EG injection.

In a second experiment, coolant injections were carried out every 2, 5 or 10 min. The performance variations over time with  $5 \mu\text{l}$  coolant injections are shown in Fig. 7(a). In CC mode of  $400 \text{ mA cm}^{-2}$ , cell performance is decreased after coolant injection, and the change of cell performance was different at the every injection time interval. The performance changes when  $1 \mu\text{l}$  was injected at various intervals (total injection time 2 h) are shown in Fig. 7(b). The same trend was observed with injection quantities of  $5 \mu\text{l}$ . The performance data of CC mode by coolant injection with  $5$  and  $1 \mu\text{l}$  are summarized in Table 2. The performance reduction of  $5 \mu\text{l}$  was larger than that of  $1 \mu\text{l}$ . Additionally, potential drop was increased with the increased coolant amount. Hence, this result is considered that periodic variation of the performance reduction and recovery is dependent by rate and amount of coolant injection.

### 3.2.2. Performance change by a strong dose of coolant

The changes in performance with large doses of coolant, i.e., rates of  $0.1$  and  $0.5 \text{ ml min}^{-1}$ , were evaluated. Coolant was injected

**Table 1**  
Characteristics of  $0.5 \mu\text{l min}^{-1}$  coolant injection experiment.

	CV	EIS (at $400 \text{ mA cm}^{-2}$ )	Polarization curve	
	ECSA (%)	Polarization resistance ( $\Omega_{\text{pol}}$ )	OCV	At $0.6 \text{ V}$
Initial	100%	0.0197	100%	100%
Coolant injection	–	0.0234	97.9%	70.5%
CC mode	–	0.0202	98.8%	92.3%
Water cleaning	91.3%	0.0199	100%	100%

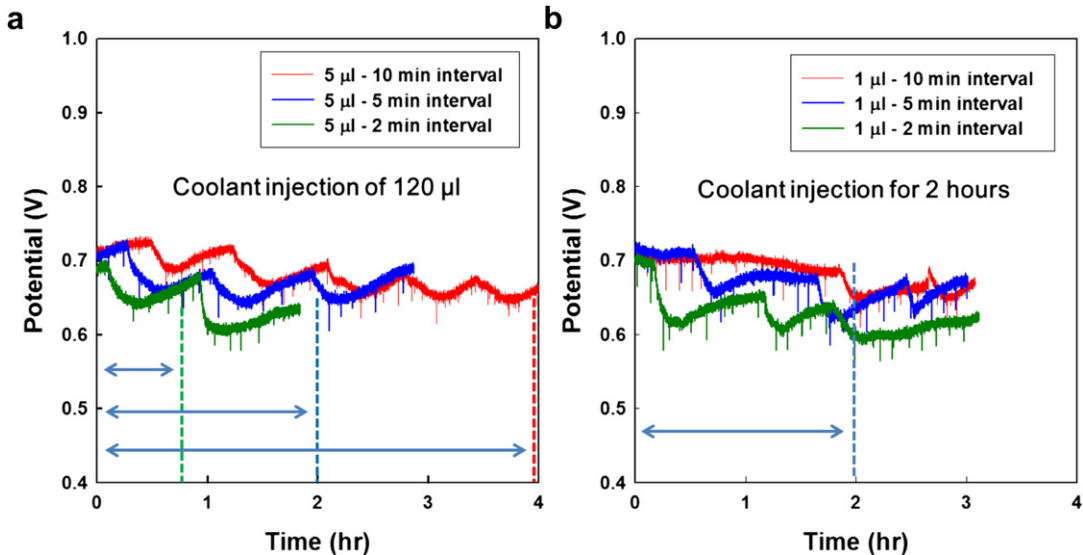


**Fig. 7.** Potential drop by coolant injection of (a) 5 and (b) 1  $\mu\text{l}$  every 10 min, 5 min, or 2 min under constant current mode ( $400 \text{ mA cm}^{-2}$ ).

**Table 2**  
Summary of coolant injection method.

Amount of injection ( $\mu\text{l}$ )	Time interval (min)	Injection time (h)	Total amount of coolant ( $\mu\text{l}$ )
5	10	4	
5	5	2	120
5	2	0.8	
1	10		12
1	5	2	24
1	2		60

in the single cell until the cell voltage fell to 0.4 V at  $400 \text{ mA cm}^{-2}$  in CC mode. The total volume of the coolant injections were about 2.3 ml (23 injections) and 6.5 ml (13 injections). Performance changes at OCV and 0.6 V are shown in Fig. 8. As shown in Fig. 8(a), OCV was observed 83% of initial value after injection of coolant at a rate of  $0.1 \text{ ml min}^{-1}$ , and it is recovered to 87.8% after in CC mode. For 1, 2, and 3 hr water cleanings, changes of OCV were observed to 97.5%, 98.6%, and 99.7%, respectively. Performance at 0.6 V dropped

to 8.0% after the injection of coolant then it was recovered to 12.8%, 57.7%, 82.0%, and 96.0% in CC mode and after water cleaning for 1 h, 2 h and 3 h, respectively. When coolant was injected at a rate  $0.5 \text{ ml min}^{-1}$ , 73.5% of the initial OCV was observed, which then recovered to 99.0% after water cleaning. At a cell voltage of 0.6 V, the performance dropped to 3% after the injection of coolant then its value was recovered to 93% after water cleaning for 3 h, as shown in Fig. 8(b). These results show that when milliliter volumes of coolant were injected into the single cell, the performance tended to be affected more by the injection frequency than by the injection amount. Fig. 9 shows the results of EIS and CV measurement. The ECSA dropped to 16.6% of the initial area after a coolant injection of  $0.1 \text{ ml min}^{-1}$ , as shown in Fig. 9(a). The ECSA was recovered to 69.0% and 92.0% after CC mode and 3-h water cleaning, respectively. The result of EIS shows that the polarization resistance was increased to 442.2% by the injection of coolant, but recovered to 109.7% after water cleaning for 3 hr. At a coolant level of  $0.5 \text{ ml min}^{-1}$ , the ECSA was reduced to 16.4%, but recovered to 59.7% and 90.0% after CC mode and water cleaning. The results of EIS show that the polarization resistance shows increase to 576.4%

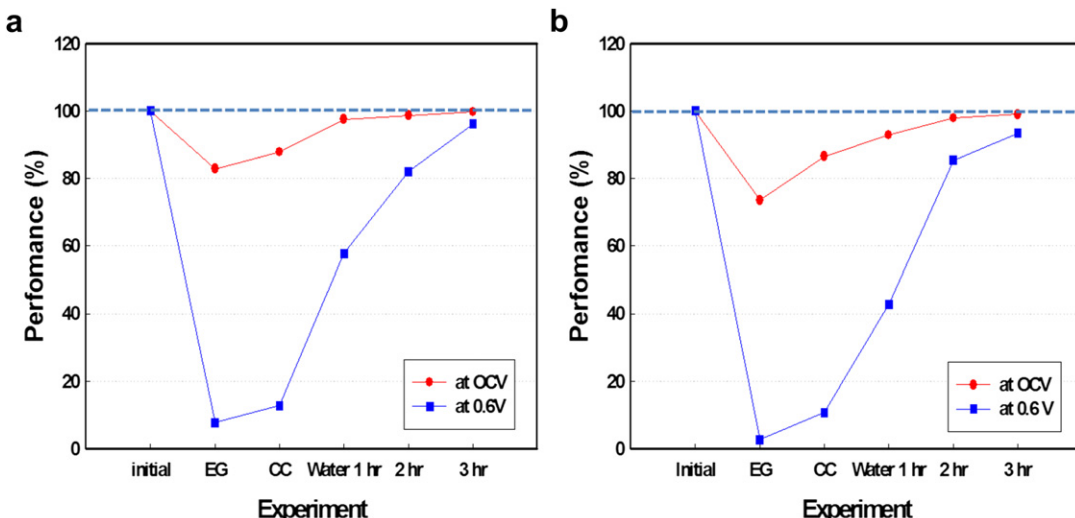


**Fig. 8.** Changes of open circuit voltage and performance at 0.6 V (a)  $0.1 \text{ ml min}^{-1}$  and (b)  $0.5 \text{ ml min}^{-1}$ .

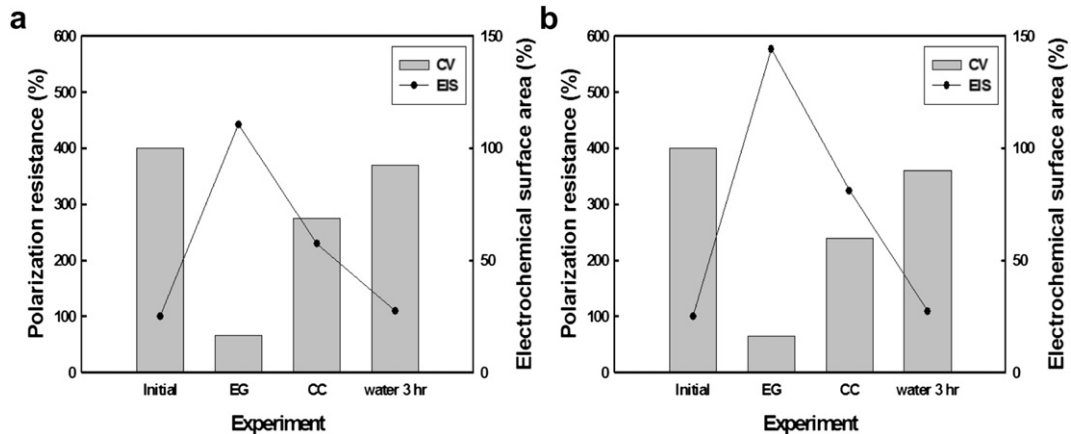


Fig. 9. Comparison by experimental condition with polarization resistance ( $\Omega$ ) and ECSA (%) (a) 0.1 and (b) 0.5  $\text{ml min}^{-1}$ .

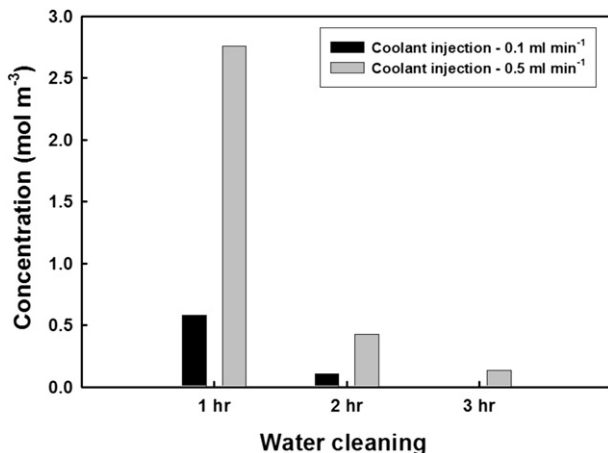


Fig. 10. Concentration of EG in vented water by GC analysis after coolant injection of 0.1 and 0.5  $\text{ml min}^{-1}$ .

after the injection of coolant, but its value was recovered to 108.9% after water cleaning, as shown in Fig. 9(b). The cell performance was not recovered to 100% because CO poisoning was generated in some Pt catalysts. Therefore, independent experiments were

conducted to determine the effects of coolant in the GDL and catalyst layer. The concentration of EG was measured by GC with washed water, as shown in Fig. 10. After water cleaning for 1 h, a high concentration of EG was confirmed to be present in both 0.1  $\text{ml min}^{-1}$  and 0.5  $\text{ml min}^{-1}$  experiments, with the concentration being higher in the 0.5  $\text{ml min}^{-1}$  experiment than in the 0.1  $\text{ml min}^{-1}$  experiment. Resistance, ECSA, and cell performance were rapidly restored with the reduction of EG concentration. This result means that physically adsorbed EG on the GDL and unreacted EG on Pt catalyst were drained.

### 3.2.3. Independent estimation of GDL and MEA

In order to investigate the influence of coolant on the GDL, the GDL at the anode side was replaced by another GDL which had been exposed to coolant for 3 h. A polarization curve of a single cell which has GDL exposed to coolant is shown in Fig. 11(a). Compared with its initial performance at 0.6 V, the performance of the exposed single cell was decreased from 850 to 600  $\text{mA cm}^{-2}$ . However, the performance was recovered to 100% after water cleaning.

In another experiment, the MEA without a GDL on the anode side was exposed to coolant for 3 h, and CC mode was operated after the MEA was reassembled into a single cell with a fresh GDL.

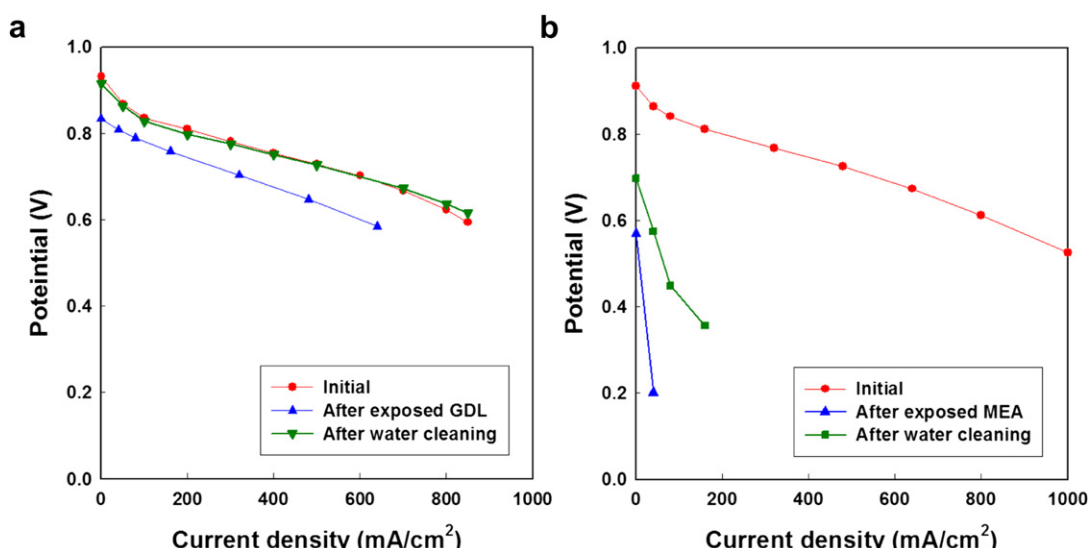
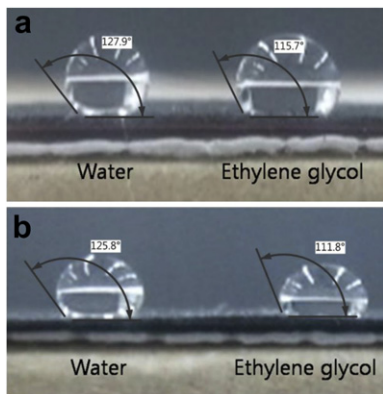


Fig. 11. Changes in polarization curve on EG solution exposed to (a) GDL and (b) MEA.



**Fig. 12.** Image of contact angle with water and EG at (a) 20 °C and (b) 65 °C.

Changes in the polarization curve when MEA was exposed are shown in Fig. 11(b). Performance of the MEA exposed in coolant was measured at 40 mA cm<sup>-2</sup> of 0.2 V and OCV of 0.57 V (fresh OCV 0.91 V). Performance was 4% of its initial value at 0.6 V after the washing process. According to the results of V. Livshits and Peled, the overpotential value at both anode and cathode was caused in an acidic environment, and its values were increased at higher current density [30]. Therefore, when coolant reached the catalyst and the membrane, performance was decreased sharply and is difficult to recover after water cleaning. These results indicate complex causes that were the CO poisoning by electro-oxidation reaction of EG on the Pt catalyst, and the interrupt of hydrogen influx by adsorbed EG at the GDL. Hence, it is considered that the cell performance was recovered by water injection due to the dissolution of EG on the GDL and the electro-oxidation reaction of water molecules on the surface of catalyst layer. Therefore, it is considered that poisoning of the Pt catalyst near the membrane side was not recovered easily by water cleaning.

The contact angle, surface tension, and viscosity of water and EG were measured to determine the adsorption on the water repellent surface of GDL. As shown in Fig. 12, Water and EG have the contact angle of 127.9 and 115.7 at 20 °C. The value was decreased to 125.8 and 111.8 at 65 °C, respectively. This result means that coolant is more easily absorbed at higher temperature due to the increased hydrophilicity. Low contact angle of GDL with strong hydrophilicity indicates a lot of adsorbed water and low gas permeability [36]. The surface tensions and viscosities of water and EG are summarized in Table 3. These results were consistent with those reported in reference [35], but EG values were measured by experiment. The surface tensions of water and EG were 72.88 and 48.43 dyn cm<sup>-1</sup> at 20 °C, respectively, and 66.23 and 44.42 dyn cm<sup>-1</sup> at 65 °C. The contact angle and surface tension of EG were reduced with increasing temperature, and were smaller than those of water at each temperature. This indicates that the physical adsorption of EG was stronger than that of water.

**Table 3**  
Summary of surface tension and viscosity of water and EG.

Temperature (°C)	Surface tension (dynes/cm)	EG <sup>b</sup>	Viscosity (cP)	EG <sup>c</sup>
20	72.88	48.43 (48.4 <sup>a</sup> )	1.002	21.0 (21 <sup>a</sup> )
65	66.23	44.42	0.434	4.8

<sup>a</sup> According to Ref. [35].

<sup>b</sup> Measured by surface tension meter.

<sup>c</sup> Measured by viscometer.

The viscosity of water and EG was measured as 1.002 and 21.0 cP at 20 °C, respectively, and 0.434 and 4.8 cP at 65 °C. The EG viscosity compared to water viscosity was about 21 times higher at 20 °C and 11 times higher at 65 °C. The viscosity of EG was decreased with increased temperature. This suggest that the physical adsorption of EG can last longer than that of water at the GDL and the adsorbed EG on the GDL can be easily cleared by water cleaning at 65 °C. These results indicate that performance is significantly affected by the physical adsorption of EG on the GDL and CO poisoning on the Pt catalyst.

#### 4. Conclusions

When coolant is injected at the anode, the performance of the PEMFC was decreased because of the poisoning of electro-oxidation reaction of EG on the Pt catalyst. The cell performance was not recovered in the CC condition. At the cathode, performance showed wave-like behavior and a small reduction, but its value was recovered in CC mode. Thus, the result considered that H<sub>2</sub>O generated on the cathode side is important for recovery of cell performance due to the electro-oxidation reaction of EG.

In this study, performance changes were observed at various time intervals (10, 5, and 2 min), rates (0.5 and 2.5 µl min<sup>-1</sup>), and amounts (0.1 and 0.5 ml min<sup>-1</sup>) of coolant injection. Periodic variation of performance reduction and recovery was indicated after injection of microliter coolant. The results show the greatest decrease in performance for the shortest examined time interval between injections (2 min). Performance was degraded by coolant leakage but recovered to over 93.0% of the initial value by deionized water cleaning. Since the ECSA of some Pt catalysts was decreased by CO poisoning, cell performance was not completely recovered. When coolant enters the cell, reduction of the ECSA is inevitable, regardless of cell performance. Using GC analysis, drain of EG was confirmed at the anode outlet. These results mean that EG can be absorbed at the GDL and thus inhibit the influx of fuel gas, which reduces performance. The physical adsorption of EG at GDL is strong due to the small contact angle, the small surface tension, and the high viscosity. An independent test with GDL and MEA was conducted. The performance of coolant-exposed GDL was recovered by water cleaning, but the performance of coolant-exposed MEA was not. Therefore, when the GDL is contaminated with coolant, performance is recover sufficiently by water cleaning without replacement with a new GDL; however, when the catalyst layer is contaminated with coolant, performance is not recover, because CO poisoning of Pt catalysts is irreversible.

#### Acknowledgment

This work was supported by Inter-Metropolitan Cooperation Development funded by the Presidential Committee on Regional Development (PCRD, Korea).

#### References

- [1] A.J. Appleby, Sci. Am. 281 (1999) 74.
- [2] A.C. Lloyd, Sci. Am. 281 (1999) 80.
- [3] C.K. Dyer, Sci. Am. 281 (1999) 88.
- [4] D.Y. Lee, S.W. Hwang, Int. J. Hydrogen Energy 33 (2009) 2790.
- [5] X. Yu, S. Ye, J. Power Sources 172 (2007) 145.
- [6] S.D. Knights, K.M. Colbow, J. St-Pierre, D.P. Wilkinson, J. Power Sources 127 (2004) 127.
- [7] D.A. Stevens, J.R. Dahn, Carbon 43 (2005) 179.
- [8] A.F. Ghenciu, Curr. Opin. Solid State Mater. Sci. 6 (2002) 389.
- [9] V. Mehta, J.S. Cooper, J. Power Sources 114 (2003) 32.
- [10] P. Costamagna, S. Srinivasan, J. Power Sources 102 (2001) 242.
- [11] F. Barbir, PEM Fuel Cells: Theory and Practice, Elsevier Academic Press, New York, 2005.
- [12] B.C.H. Steele, A. Heinzel, Nature 414 (2001) 345–352.

[13] R.F. Service, Science 305 (2004) 958.

[14] J. Larminie, A. Dicks, Fuel Cell Systems Explained, second ed., John Wiley & Sons Inc, 2003.

[15] S.G. Kangm, K.D. Min, F. Mueller, J. Brouwer, Int. J. Hydrogen Energy 34 (2010) 6749–6764.

[16] B. Wieland, J.P. Lancaster, C.S. Hoaglund, P. Holota, W.J. Tornquist, Langmuir 12 (1996) 2594.

[17] M.J. Gonzales, C.T. Hable, M.S. Wrighton, J. Phys. Chem. B 102 (1998) 9881–9890.

[18] R.B. de Lima, V. Paganin, T. Iwasita, W. Vielstich, Electrochim. Acta 49 (2003) 85.

[19] K. Matsuoka, Y. Iriyama, T. Abe, M. Matsuoka, Z. Ogumi, Electrochim. Acta 51 (2005) 1085.

[20] K. Matsuoka, Y. Iriyama, T. Abe, M. Matsuoka, Z. Ogumi, J. Power Sources 150 (2005) 27.

[21] J.D. Kim, Y.I. Park, K. Kobayashi, M. Nagai, M. Kunitatsu, Solid State Ionic 140 (2001) 313.

[22] S. Jimenez, J. Soler, R.X. Valenzuela, L. Daza, J. Power Sources 151 (2005) 69.

[23] B. Wu, Y. Gao, G. Li, W. Qu, Z. Jiang, Catal. Lett. 106 (2006) 3.

[24] S.M. Choi, M.H. Seo, H.J. Kim, E.J. Lim, W.B. Kim, Int. J. Hydrogen Energy 35 (2010) 6853–6862.

[25] A.H. Thomason, T.T. Lalk, A.J. Appleby, J. Power Sources 135 (2004) 204–211.

[26] W.A. Adams, J. Blair, K.R. Bullock, C.L. Gardner, J. Power Sources 145 (2005) 55–61.

[27] Z. Qi, C. He, A. Kaufman, J. Power Sources 111 (2002) 239.

[28] Z. Xu, Z. Qi, A. Kaufman, J. Power Sources 156 (2006) 281.

[29] D.J.L. Brett, S. Atkins, N.P. Brandon, V. Vesovic, N. Vasileiadis, A.R. Kucernak, J. Power Sources 133 (2004) 205.

[30] V. Livshits, E. Peled, J. Power Sources 161 (2006) 1187.

[31] V. Livshits, M. Philosoph, E. Peled, J. Power Sources 178 (2008) 687.

[32] F.A. de Bruijn, D.C. Papageorgopoulos, E.F. Sitters, G.J.M. Janssen, J. Power Sources 110 (2002) 117.

[33] G.J.M. Janssen, J. Power Sources 136 (2004) 45.

[34] V.P. Carey, Liquid-vapor Phase-change Phenomena, Taylor & Francis, London, 1992.

[35] N.A. Lange, Lange's Handbook of Chemistry, thirteenth ed., McGraw-Hill Co, 1985.

[36] J.H. Chun, K.T. Park, D.H. Jo, J.Y. Lee, S.G. Kim, S.H. Park, E.S. Lee, J.Y. Jyoung, S.H. Kim, J. Power Sources 36 (2011) 8422.

[37] V. selvaraj, M. Vinoba, M. Alagar, J. Colloid Interf. Sci. 332 (2008) 537–544.

[38] A. Servo, C. Kwak, Appl. Catal. B Environ. 97 (2010) 1–12.